A practical leader-follower tracking control scheme for multiple nonholonomic mobile robots in unknown obstacle environments

Wang, Yuanzhe; Wang, Danwei; Yang, Shuai; Shan, Mao

2018

Wang, Y., Wang, D., Yang, S., & Shan, M. (2019). A practical leader-follower tracking control scheme for multiple nonholonomic mobile robots in unknown obstacle environments. IEEE Transactions on Control Systems Technology, 27(4), 1685-1693. doi:10.1109/tcst.2018.2825943

https://hdl.handle.net/10356/137402

https://doi.org/10.1109/TCST.2018.2825943

A Practical Leader-Follower Tracking Control Scheme for Multiple Nonholonomic Mobile Robots in Unknown Obstacle Environments

Yuanzhe Wang, Danwei Wang, *Senior Member, IEEE*, Shuai Yang, and Mao Shan, *Member, IEEE*

***Abstract*—This brief addresses the leader-follower ($L-F$) tracking control problem for multiple nonholonomic mobile robots in unknown obstacle environments. Unlike most of the existing approaches investigating similar problems, a series of practical issues are considered and tackled in the proposed scheme. For leader tracking, a class of bounded barrier functions are employed to formulate distance and bearing angle constraints introduced by sensor limitations and $L-F$ collision avoidance requirement. To ensure robot safety in unknown environments, a multi-region obstacle avoidance algorithm is proposed which prioritizes different control objectives in different regions. This brief also studies the leader-loss situation, which may be caused by illumination variation, motion blurring or visual occlusion by obstacles. To deal with this case, a fault-tolerant strategy is designed to drive F to the place where L was lost immediately. The control scheme proposed in the brief is primarily designed for a communication-free environment where only local state measurements are available. Furthermore, it has control input constraints explicitly taken into account. Real robot experiment has been performed to validate the proposed method.**

***Index Terms*—Mobile robots, leader-follower, formation control, obstacle avoidance, constrained control, fault-tolerant control.**

I. Introduction

Multi-robot systems have wide applications in both civilian and military fields, such as coordinated target tracking, sensitive area surveillance and unknown environment exploration. Formation keeping, which is one of the main objectives for multi-robot control, has been investigated extensively in the past decade (see [1] for an in-depth survey). As a result, a large variety of formation control approaches have emerged [2]–[5], among which leader-follower ($L-F$) approach is preferable due to its simplicity and scalability in practical applications. However, most of the existing $L-F$ approaches are subject to certain limitations when implemented for addressing real formation control problems, mainly due to additional constraints including sensor limitations, obstacle and inter-robot collision avoidance in unknown environments, communication-free environment, unavailability of global state measurements, control input constraints, leader-loss situation and so forth. From the viewpoint of developing a feasible control strategy for practical applications, this brief mainly focuses on three practical issues: sensor limitations, obstacle and inter-robot collision avoidance in unknown environments and leader-loss situation.

For $L-F$ formation implementation, stereo camera is generally employed for F to detect L. However, stereo cameras are generally subject to limited depth range and field-of-view (FOV), resulting in the maximum and minimum distance requirements between F and L as well as the bearing angle constraints of L with respect to F. Violation of such constraints will lead to loss of detection. Even though it is considered critical, few researchers have paid attention to this issue. Sensory limitations are taken into account in [6], however, they are merely used to determine the neighbors of a vehicle. In [7], time-varying *tan*-type barrier Lyapunov functions are introduced to characterize the line-of-sight (LOS) range and angle constraints. However, the LOS range and angle are defined with respect to the global coordinate frame and cannot be used to describe stereo camera limitations. Reference [8] proposes a generalized *tan*-type barrier Lyapunov function to formulate the detection range and FOV limitations of the sensor. However, the value of the barrier function employed approaches infinity when the constraints are close to being violated, resulting in unbounded control inputs.

The second issue is concerned with the obstacle and inter-robot collision avoidance in unknown environments. Safety is considered as the foremost issue for any control problems. For multi-robot formation applications, obstacle and inter-robot collision avoidance is closely related to system safety and therefore should hold the highest priority among all the objectives, meaning that the formation objective should be compromised when conflicting with collision avoidance. Important as this issue is, most of the existing formation control approaches have not fully taken into account the obstacle avoidance problem. References [9], [10] are two successful attempts with real robot demonstrations, however, they only treat point or disk obstacles in their simulations and experiments, which is unrealistic in applications where robots work in an unstructured environment. Even though [11] designs a behavior-based algorithm for inter-robot collision avoidance with experimental validations, the proposed method is incapable of avoiding static obstacles. There are also some results like [12]–[14] aiming at solving obstacle and inter-agent collision avoidance problem for multi-agent formations. Yet those methods are all based on global position measurements, making them not applicable for situations where only

Y. Wang, D. Wang and S. Yang are with the School of Electrical and Electronic Engineering, Nanyang Technological University, 639798 Singapore (e-mail: wang0951@e.ntu.edu.sg; edwwang@ntu.edu.sg; yang0392@e.ntu.edu.sg).

M. Shan is with the Australian Centre for Field Robotics, The University of Sydney, Sydney, NSW 2006, Australia (e-mail: m.shan@acfr.usyd.edu.au).

local state measurements are available. Besides, their validity has not been well supported by experiment results.

The third issue is about the leader-loss situation. To date, there are already many research outcomes trying to solve the visibility maintenance problem for multi-robot systems. However, maintaining visibility between L and F particularly in unknown obstacle environments is of great difficulty since occlusion of LOS visibility by obstacles is inevitable. Besides, camera detection may temporarily malfunction in operation, attributed to change of lighting condition, motion blurring, etc. Thus, from the practical point of view, the leader-loss situation should be taken into consideration and fault-tolerant strategies able to recover visibility should be designed. Although there are already a few literatures on LOS/visibility maintenance for $L-F$ formations like [15]–[18], they are under the assumption that the visual detection is reliable. Besides, they either do not consider the presence of obstacles or assume that the environment information is known *a priori*.

In this brief, a practical tracking control scheme is proposed for $L-F$ nonholonomic mobile robots moving in unknown obstacle environments. Sensor limitations, including the depth range and FOV constraints, are formulated by a class of bounded barrier functions, which are then incorporated into the control law. Collision avoidance between L and F is also described as a minimum range constraint and solved simultaneously. For the safety consideration of the robot in unknown environments, a multi-region obstacle avoidance algorithm is proposed where different control objectives are given the uppermost priority in different regions. This brief also considers the leader-loss case in which the visibility is broken due to obstacles, change of lighting condition or motion blurring. To tackle this situation, a fault-tolerant strategy is designed such that F will move to the place where L was lost as soon as possible. The proposed approach uses only local state measurements obtained by stereo camera mounted on F in a communication-free environment, and takes into account control input constraints explicitly. Finally, real robot experimental results are presented to validate the efficacy of the proposed control method.

The main contributions of this brief are listed as follows:

1) A leader-tracking control law is proposed which takes sensor constraints explicitly into account.
2) A multi-region obstacle avoidance algorithm is designed to guarantee the robot safety in unknown environments.
3) The leader-loss situation is pointed out while the corresponding analysis and a fault-tolerant solution are provided.
4) Real robot experiment has been performed to demonstrate the effectiveness of the proposed control method.

The remainder of this brief is organized as follows. In Section II, the problem is formulated. Section III provides the main results. Experimental results are given in Section IV, while final conclusions and future works are stated in Section V.

II. Problem Formulation

This brief considers a typical application where two differential-drive wheeled mobile robots move in a 2D workspace with unknown obstacles, using vision-based $L-F$ techniques. It is assumed that one of the robots, defined as L, moves autonomously in the workspace without communication between the robots, while the other one acts as F tracking L and performing obstacle and inter-robot collision avoidance subject to sensor limitations and control input constraints. The problem can be generalized to a snakelike multi-robot formation with $N > 2$ members.

A. Modeling of the $L-F$ pair

The kinematic model of the robots is given as follows.

$$\dot{x}_i = v_i \cos\theta_i,\ \dot{y}_i = v_i \sin\theta_i,\ \dot{\theta}_i = \omega_i, \tag{1}$$

where $i \in \{L, F\}$, $\mathbf{p}_i = [x_i, y_i]^T \in \mathbf{R}^2$ and θ_i are the position and heading angle of robot i with respect to the global coordinate frame $\{G\} = \{\vec{x}_G, \vec{y}_G\}$, respectively, while v_i and ω_i are the linear velocity and angular velocity of robot i, respectively, in its corresponding body-fixed local frame $\{i\} = \{\vec{x}_i, \vec{y}_i\}$.

It is assumed that F is equipped with a stereo camera which can detect the relative position including distance and bearing angle of L with respect to $\{F\}$. The relative position relationship between L and F is depicted in Fig. 1(a). To facilitate analysis, polar coordinates are used to describe the relative position relationship.

The distance ρ between L and F as well as the bearing angle α of L with respect to $\{F\}$ are defined as

$$\rho = \|\mathbf{p}_L - \mathbf{p}_F\|_2,\ \alpha = \arctan 2(\tilde{y}_L, \tilde{x}_L), \tag{2}$$

where $\arctan 2(y, x)$ is the arctangent function with two arguments returning the appropriate quadrant of the angle of point (x, y) as a numeric value in the range $(-\pi, \pi]$. Moreover, $(\tilde{x}_L, \tilde{y}_L)$ is the Cartesian coordinates of L with respect to $\{F\}$, i.e., $\begin{bmatrix} \tilde{x}_L \\ \tilde{y}_L \end{bmatrix} = \begin{bmatrix} \cos\theta_F & \sin\theta_F \\ -\sin\theta_F & \cos\theta_F \end{bmatrix} \begin{bmatrix} x_L - x_F \\ y_L - y_F \end{bmatrix}$.

As is assumed above, ρ and α can be obtained by the stereo camera. Following some straightforward calculations, the dynamics of ρ and α can be given as

$$\begin{aligned} \dot{\rho} &= -v_F \cos\alpha + v_L \cos(\theta_L - \theta_F - \alpha), \\ \dot{\alpha} &= -\omega_F + \frac{v_F}{\rho}\sin\alpha + \frac{v_L}{\rho}\sin(\theta_L - \theta_F - \alpha). \end{aligned} \tag{3}$$

According to the physical meanings of ρ and α, $\rho \in (0, +\infty)$ and $\alpha \in (-\pi, \pi]$.

B. Modeling of the system constraints

Considering the limited depth range and FOV of the stereo camera which are described in Fig. 1(a), to avoid loss of detection, ρ must be smaller than the maximum detection range d_{max} and larger than the minimum detection range d_{min}, besides, α should be restricted in a specific range $[\alpha_{min}, \alpha_{max}]$. Furthermore, to guarantee collision-free between L and F, ρ should be larger than the safe distance d_{safe}. Therefore, the constraints on ρ and α can be given as follows.

$$\rho \in [\rho_{min}, \rho_{max}],\ \alpha \in [\alpha_{min}, \alpha_{max}], \tag{4}$$

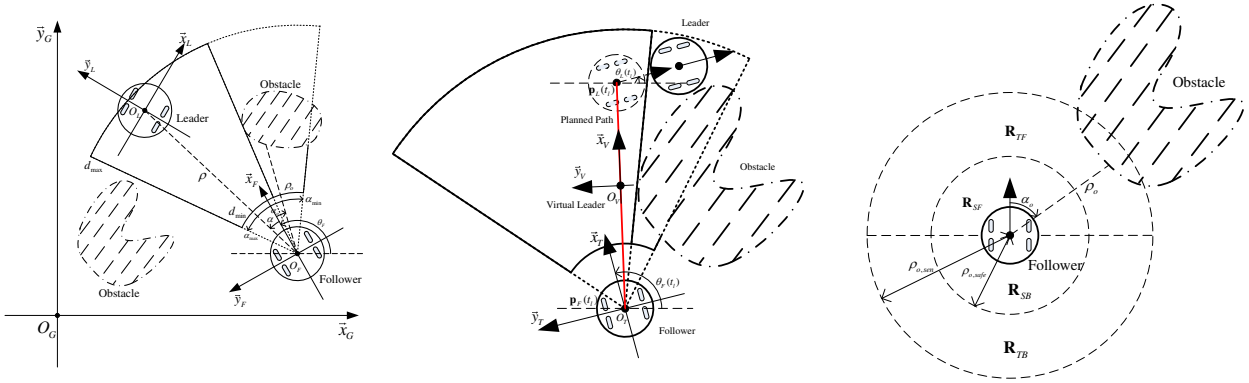

(a) $L-F$ setup with obstacles (b) Leader-loss example (c) The diagram of obstacle avoidance

Fig. 1. Illustrative diagrams

where $\rho_{min} = \max\{d_{min}, d_{safe}\}$ and $\rho_{max} = d_{max}$. From the discussions above, it can be found that ρ_{min}, ρ_{max}, α_{min}, α_{max} are constant parameters determined by sensor limitations and safety requirement.

For the purpose of obstacle avoidance, the local position of the obstacle measured in $\{F\}$ is also defined. Similarly, the distance between the obstacle and F is defined as ρ_o and the bearing angle of the obstacle measured in $\{F\}$ is defined as α_o. It is assumed that a sufficient condition for obstacle avoidance is given as

$$\rho_o \geq \rho_{o,safe}, \tag{5}$$

where $\rho_o = \|\mathbf{p}_F - \mathbf{p}_o\|_2$, $\forall \mathbf{p}_o \in \mathscr{O}$, $\mathscr{O}$ is a set of all the points on obstacles in the workspace, $\rho_{o,safe}$ is the safe distance which should be determined by taking into account the robot size. In this brief, the robot can get ρ_o using a stereo camera or a laser range finder. The relative position relationship between the robots and the obstacles is also shown in Fig. 1(a).

Finally, for real robots, the linear velocity and angular velocity are bounded due to electromechanical limitations. Therefore, L and F are subject to the following control input constraints.

$$|v_L| \leq \bar{v}_L, \ \ |\omega_L| \leq \bar{\omega}_L, \ \ |v_F| \leq \bar{v}_F, \ \ |\omega_F| \leq \bar{\omega}_F, \tag{6}$$

where $\bar{v}_L$ and $\bar{\omega}_L$ are the bounds of v_L and ω_L, respectively, while $\bar{v}_F$ and $\bar{\omega}_F$ are the bounds of v_F and ω_F, respectively.

C. Modeling of the leader-loss situation

As previously stated in the introduction, the obstacle avoidance behavior may break the distance and bearing angle constraints, resulting in loss of detection of L, while environment interference and motion blurring could also cause the leader-loss consequence. Therefore, visibility of L cannot be constantly maintained in practical applications. A leader-loss example is presented in Fig. 1(b), where L is occluded by the obstacle. This subsection will formulate the leader-loss problem.

Before going on, picture a scenario where a policeman is pursuing a thief in a cluttered environment. The thief suddenly turns at a corner and disappears in front of the policeman. An intuitive reaction of the policeman is to reach the spot where the thief was last seen, as quickly as possible, in the hope of continuing the pursuit. Inspired by such a human nature reaction, a fault-tolerant strategy to the target-loss situation should consist of two steps. The first step is to find the shortest path for F from the current state to the goal state, which is actually the last detected leader state. The second step is to control F to move along the path to the goal state as fast as possible.

To design the fault-tolerant strategy, it should be noted that this brief is under the assumption that global state feedback is not available, that is, the global states of L and F at t_l, which is the time instant when the leader was lost, cannot be obtained. To design the algorithm, a temporary coordinate frame $\{T\} = \{\vec{x}_T, \vec{y}_T\}$ is defined which is coincident with the local frame $\{F\}$ at time t_l, i.e., $\{T\} = \{F\}|_{t=t_l}$. As the movement range for the leader-loss reaction is relatively small, the accuracy of the odometry mounted on F should be within tolerance. Consequently, the odometry measurements can be utilized in the algorithm design as the state feedback with respect to $\{T\}$.

From the analysis stated above, the objective of the fault-tolerant strategy is to plan the shortest path ${}^T\mathbf{p}_V(l)$ from the starting state $({}^T\mathbf{p}_F(t_l), {}^T\theta_F(t_l))$ to the goal state $({}^T\mathbf{p}_L(t_l), {}^T\theta_L(t_l))$, where l is the arc length parameter, $({}^T\mathbf{p}_F(t_l), {}^T\theta_F(t_l))$ and $({}^T\mathbf{p}_L(t_l), {}^T\theta_L(t_l))$ are the states of F and L measured at t_l with respect to $\{T\}$ respectively, and design a control law such that F can reach the goal state along the planned path as fast as possible.

Based on the discussions above, the $L-F$ tracking control problem concerned in this brief can be formulated as follows.

Problem 1. *($L-F$ tracking control). Consider a $L-F$ pair described by (1) moving in an unknown obstacle environment. Assume that L moves autonomously in the workspace, the robots cannot communicate with each other and only local state measurements are available. Design a control scheme for F such that*

1) *(Leader tracking). When there are no obstacles nearby, ρ and α converge to the neighborhoods of the desired values ρ_d and α_d, respectively, while ensuring that the constraints (4) and (6) will not be violated during operation.*

2) *(Obstacle avoidance). The condition (5) and the constraint (6) will always be satisfied.*
3) *(Leader-loss reaction). When L cannot be detected, F will move from the starting state $({}^T\mathbf{p}_F(t_l), {}^T\theta_F(t_l))$ to the goal state $({}^T\mathbf{p}_L(t_l), {}^T\theta_L(t_l))$ along the planned path ${}^T\mathbf{p}_V(l)$ while (5) and (6) will always be guaranteed.*

To facilitate the discussion of the main results, the following lemmas are stated.

Lemma 1. *For any $\alpha, \beta \in \mathbf{R}$, the following inequality always holds,*

$$\left|\frac{\sin\alpha - \sin\beta}{\alpha - \beta}\right| \leq 1.$$

Proof: According to the sum-to-product trigonometric identities, it can be obtained that $\frac{\sin\alpha-\sin\beta}{\alpha-\beta} = \sin(\frac{\alpha-\beta}{2})\cos(\frac{\alpha+\beta}{2})/\frac{\alpha-\beta}{2}$.

Before determining the upper bound of $\frac{\sin\alpha-\sin\beta}{\alpha-\beta}$, the upper bound of function $f(x) = \frac{\sin x}{x}$ should be derived. The derivative of $f(x)$ with respect to x is $f'(x) = \frac{g(x)}{x^2}$, where $g(x) = x\cos x - \sin x$. As the derivative of $g(x)$ with respect to x is $g'(x) = -x\sin x \leq 0$, it is obvious that $g(x) \leq g(0) = 0$, $\forall x \geq 0$. Consequently, $f'(x) \leq 0$, $\forall x \geq 0$, which implies that $f(x) \leq f(0) = 1$, $\forall x \geq 0$. As $f(x)$ is an even function and $f(x) > 0$, $f(x) \in (0, 1]$. Therefore, it can be concluded that $\left|\frac{\sin\alpha-\sin\beta}{\alpha-\beta}\right| \leq \left|\sin(\frac{\alpha-\beta}{2})/\frac{\alpha-\beta}{2}\right| \left|\cos(\frac{\alpha+\beta}{2})\right| \leq 1$. ∎

Lemma 2. *For any $x \in \mathbf{R}$, the following inequality always holds,*

$$\left|\tanh(x)[1 - \tanh^2(x)]\right| \leq \frac{2\sqrt{3}}{9}.$$

Proof: Let $f(x) = \tanh(x)[1 - \tanh^2(x)]$. Taking the differentiation of $f(x)$ with respect to x yields $f'(x) = [1 - \tanh^2(x)][1 - 3\tanh^2(x)]$. As $\tanh(x) \in (-1, 1)$, it can be concluded that when $\tanh^2(x) \geq \frac{1}{3}$, $f'(x) \leq 0$, and when $\tanh^2(x) < \frac{1}{3}$, $f'(x) > 0$. As $f(x) \to 0$ when $x \to \pm\infty$, $|f(x)| \leq \frac{2\sqrt{3}}{9}$. ∎

III. Main Results

This section presents the main results. First, the leader tracking problem with distance and bearing angle constraints is studied, then a control law is proposed. Next, a multi-region obstacle avoidance algorithm is presented. Finally, the leader-loss situation is discussed and a fault-tolerant strategy is designed.

A. Leader tracking

In this subsection, a control scheme is proposed to solve the leader tracking problem under sensor limitations while collision avoidance between L and F is also guaranteed. To facilitate the discussion about the system constraints, the following bounded barrier functions are introduced to describe the constraints for ρ and α.

$$B_\rho(\rho) = \begin{cases} \beta_\rho \frac{(\rho-\rho_d)^2}{(\rho_{max}-\rho_d)^2}, & \rho_d < \rho \leq \rho_{max} \\ \beta_\rho \frac{(\rho-\rho_d)^2}{(\rho_d-\rho_{min})^2}, & \rho_{min} \leq \rho \leq \rho_d \end{cases}, \quad (7)$$

$$B_\alpha(\alpha) = \begin{cases} \beta_\alpha \frac{(\alpha-\alpha_d)^2}{(\alpha_{max}-\alpha_d)^2}, & \alpha_d < \alpha \leq \alpha_{max} \\ \beta_\alpha \frac{(\alpha-\alpha_d)^2}{(\alpha_d-\alpha_{min})^2}, & \alpha_{min} \leq \alpha \leq \alpha_d \end{cases}, \quad (8)$$

where β_ρ and β_α are the design parameters whose values are equal to $B_\rho(\rho_{max})$, $B_\rho(\rho_{min})$ and $B_\alpha(\alpha_{max})$, $B_\alpha(\alpha_{min})$ respectively. It can be found that $B_\rho(\rho)$ has the minimum value 0 at ρ_d and increases monotonically to the maximum value β_ρ when ρ approaches ρ_{min} or ρ_{max}. Similar results also hold for $B_\alpha(\alpha)$.

In the sequel, the barrier functions (7) and (8) will be employed to develop a control law that can drive F to track L under distance and bearing angle constraints. In this brief, it is assumed that $\bar{v}_L$ is known to F. This assumption is reasonable, because v_L must be smaller than v_F, otherwise, F cannot catch up with L. Based on the discussions above, the following control law is proposed for F.

$$\begin{aligned} v_F &= \frac{1}{\cos\alpha}[k_\rho \nabla B_\rho + \bar{v}_L \tanh(\frac{\bar{v}_L \nabla B_\rho}{\delta_\rho})], \\ \omega_F &= \frac{v_F}{\rho}\sin\alpha + \frac{\bar{v}_L}{\rho}\tanh(\frac{\bar{v}_L \nabla B_\alpha}{\rho\delta_\alpha}) + k_\alpha \nabla B_\alpha, \end{aligned} \quad (9)$$

where k_ρ, k_α, δ_ρ and δ_α are positive constant parameters, ∇B_ρ and ∇B_α are the gradients of B_ρ and B_α with respect to ρ and α, respectively. In addition, k_ρ, k_α, δ_ρ and δ_α satisfy the following conditions.

$$\begin{aligned} & k_\rho \leq \tfrac{\bar{v}_F\xi_\rho - \bar{v}_L}{G_\rho}, \\ & k_\alpha \leq \tfrac{\bar{\omega}_F\rho_{min} - \bar{v}_L - \bar{v}_F\xi_\alpha}{G_\alpha\rho_{min}}, \\ & \rho_d - \tfrac{(\rho_{min}-\rho_d)^2}{2\beta_\rho}\sqrt{\tfrac{k_p\delta_\rho}{k_\rho}} > \rho_{min}, \\ & \rho_d + \tfrac{(\rho_{max}-\rho_d)^2}{2\beta_\rho}\sqrt{\tfrac{k_p\delta_\rho}{k_\rho}} < \rho_{max}, \\ & \alpha_d - \tfrac{(\alpha_{min}-\alpha_d)^2}{2\beta_\alpha}\sqrt{\tfrac{k_p\delta_\alpha}{k_\alpha}} > \alpha_{min}, \\ & \alpha_d + \tfrac{(\alpha_{max}-\alpha_d)^2}{2\beta_\alpha}\sqrt{\tfrac{k_p\delta_\alpha}{k_\alpha}} < \alpha_{max}, \end{aligned} \quad (10)$$

where $\xi_\rho = \min\{\cos\alpha_{min}, \cos\alpha_{max}\}$, $G_\rho = \max\{\frac{2\beta_\rho}{\rho_{max}-\rho_d}, \frac{2\beta_\rho}{\rho_d-\rho_{min}}\}$, $\xi_\alpha = \min\{\sin\alpha_{min}, \sin\alpha_{max}\}$ and $G_\alpha = \max\{\frac{2\beta_\alpha}{\alpha_{max}-\alpha_d}, \frac{2\beta_\alpha}{\alpha_d-\alpha_{min}}\}$.

The above discussions lead to the following theorem which proves that the proposed control law can drive F to maintain a flexible distance and bearing angle with L while the distance and bearing angle constraints are not violated during operation. In the meantime, the control input constraints are satisfied as well.

Theorem 1. *Consider a $L - F$ robot pair modeled by (1). Assume that L moves autonomously with v_L bounded by $\bar{v}_L$ and the constraints (4) is satisfied at the initial time. Using the proposed control law (9) where the parameters are chosen according to (10), the following results can be achieved.*

1) *ρ will converge to $\{\rho | \rho_d - \frac{(\rho_{min}-\rho_d)^2}{2\beta_\rho}\sqrt{\frac{k_p\delta_\rho}{k_\rho}} < \rho < \rho_d + \frac{(\rho_{max}-\rho_d)^2}{2\beta_\rho}\sqrt{\frac{k_p\delta_\rho}{k_\rho}}\}$ asymptotically while α will asymptotically converge to $\{\alpha | \alpha_d - \frac{(\alpha_{min}-\alpha_d)^2}{2\beta_\alpha}\sqrt{\frac{k_p\delta_\alpha}{k_\alpha}} < \alpha < \alpha_d + \frac{(\alpha_{max}-\alpha_d)^2}{2\beta_\alpha}\sqrt{\frac{k_p\delta_\alpha}{k_\alpha}}\}$.*
2) *The constraints (4) will not be violated during operation.*
3) *The constraints (6) will always be satisfied.*

Proof: First, consider Lyapunov function candidate $V_\rho = B_\rho$. Then, from (3) and (9), it can be obtained that

$$\dot{\rho} = -k_\rho \nabla B_\rho - \bar{v}_L \tanh(\frac{\bar{v}_L \nabla B_\rho}{\delta_\rho}) + v_L \cos(\theta_L - \theta_F - \alpha).$$

According to the above equations, it can be derived that

$$\begin{aligned}\dot{V}_\rho =& - k_\rho (\nabla B_\rho)^2 - \bar{v}_L \nabla B_\rho \tanh(\frac{\bar{v}_L \nabla B_\rho}{\delta_\rho}) \\ &+ v_L \nabla B_\rho \cos(\theta_L - \theta_F - \alpha) \\ \leq& - k_\rho (\nabla B_\rho)^2 - \bar{v}_L \nabla B_\rho \tanh(\frac{\bar{v}_L \nabla B_\rho}{\delta_\rho}) + \bar{v}_L |\nabla B_\rho|\end{aligned}.$$

Based on Lemma 1 of [8], it can be got that $\dot{V}_\rho \leq -k_\rho (\nabla B_\rho)^2 + k_p \delta_\rho$. Thus, when $(\nabla B_\rho)^2 > \frac{k_p \delta_\rho}{k_\rho}$, $\dot{V}_\rho < 0$. Therefore, ρ will converge into $\{\rho | (\nabla B_\rho)^2 > \frac{k_p \delta_\rho}{k_\rho}\}$, i.e. $\{\rho | \rho_d - \frac{(\rho_{min} - \rho_d)^2}{2\beta_\rho} \sqrt{\frac{k_p \delta_\rho}{k_\rho}} < \rho < \rho_d + \frac{(\rho_{max} - \rho_d)^2}{2\beta_\rho} \sqrt{\frac{k_p \delta_\rho}{k_\rho}}\}$, asymptotically. Based on condition (10), the above set does not violate the distance constraint (4).

Meanwhile, consider Lyapunov function candidate $V_\alpha = B_\alpha$. It can be derived from (3) and (9) that

$$\dot{\alpha} = -k_\alpha \nabla B_\alpha - \frac{\bar{v}_L}{\rho} \tanh(\frac{\bar{v}_L \nabla B_\alpha}{\rho \delta_\alpha}) + \frac{v_L}{\rho} \sin(\theta_L - \theta_F - \alpha).$$

Differentiating V_α with respect to time yields

$$\begin{aligned}\dot{V}_\alpha =& - k_\alpha (\nabla B_\alpha)^2 - \frac{\bar{v}_L \nabla B_\alpha}{\rho} \tanh(\frac{\bar{v}_L \nabla B_\alpha}{\rho \delta_\alpha}) \\ &+ \frac{v_L \nabla B_\alpha}{\rho} \sin(\theta_L - \theta_F - \alpha) \\ \leq& - k_\alpha (\nabla B_\alpha)^2 - \frac{\bar{v}_L \nabla B_\alpha}{\rho} \tanh(\frac{\bar{v}_L \nabla B_\alpha}{\rho \delta_\alpha}) + \frac{\bar{v}_L |\nabla B_\alpha|}{\rho}\end{aligned}.$$

According to Lemma 1 of [8], it is easy to obtain $\dot{V}_\alpha \leq -k_\alpha (\nabla B_\alpha)^2 + k_p \delta_\alpha$, which implies that when $(\nabla B_\alpha)^2 > \frac{k_p \delta_\alpha}{k_\alpha}$, $\dot{V}_\alpha < 0$. Consequently, α will converge into $\{\alpha | (\nabla B_\alpha)^2 > \frac{k_p \delta_\alpha}{k_\alpha}\}$, i.e. $\{\alpha | \alpha_d - \frac{(\alpha_{min} - \alpha_d)^2}{2\beta_\alpha} \sqrt{\frac{k_p \delta_\alpha}{k_\alpha}} < \alpha < \alpha_d + \frac{(\alpha_{max} - \alpha_d)^2}{2\beta_\alpha} \sqrt{\frac{k_p \delta_\alpha}{k_\alpha}}\}$, asymptotically. It can be easily verified that the above set also satisfies the bearing angle constraints (4).

Thus 1) has been proven.

Next, the distance and bearing angle constraints will be analyzed. For the distance constraints, when $\rho \to \rho_{max}^-$, $\dot{B}_\rho < 0$. As $\dot{B}_\rho = \dot{\rho} \nabla B_\rho$ and $\nabla B_\rho > 0$ when $\rho \to \rho_{max}^-$, $\dot{\rho} < 0$. And when $\rho \to \rho_{min}^+$, $\dot{B}_\rho < 0$. As $\nabla B_\rho < 0$ when $\rho \to \rho_{min}^+$, $\dot{\rho} > 0$. This means that when ρ approaches the upper or the lower bound, the control law will drive F such that ρ decreases to avoid exceeding the bound. Similarly, it can also be concluded that when α is about to violate the constraints, the control law will react to keep α within the given range.

Finally, the control input constraints will be analyzed. From (9), it is obvious that $|v_F| \leq \frac{1}{\xi_\rho} k_\rho |\nabla B_\rho| + \frac{1}{\xi_\rho} \bar{v}_L$. From (7), it can be easily obtained that $|\nabla B_\rho| \leq G_\rho$. Thus, combined with (10), $|v_F| \leq \bar{v}_F$ is satisfied. Similarly, from (9), $|\omega_F| \leq \frac{\bar{v}_F}{\rho_{min}} \xi_\alpha + \frac{\bar{v}_L}{\rho_{min}} + k_\alpha |\nabla B_\alpha|$. From (8), it can be found that $|\nabla B_\alpha| \leq G_\alpha$. Thus, according to (10), $|\omega_F| \leq \bar{\omega}_F$ can also be guaranteed.

This completes the proof. ■

B. Unknown obstacle avoidance

The previous subsection addresses the leader tracking problem in an obstacle-free environment. However, in many practical applications, the obstacle information is out-of-date or even unavailable to the robots because of obstacles not detected beforehand, and/or new random obstacles in the operation. Therefore, an algorithm for unknown obstacle avoidance should be designed to guarantee the safety of the robots.

Before going on, the relative position relationship between F and the obstacle is analyzed and depicted in Fig. 1(c). In our algorithm, F only considers the nearest obstacle around it and a set of regions are defined according to the relative position of the nearest obstacle with respect to $\{F\}$, which are front transition region $\mathbf{R}_{TF}$, back transition region $\mathbf{R}_{TB}$, front safe region $\mathbf{R}_{SF}$ and lastly back safe region $\mathbf{R}_{SB}$. Mathematically, these four regions are defined as

$$\begin{aligned}\mathbf{R}_{TF} &\triangleq \{\mathbf{p}' | \rho_{o,safe} < \rho' \leq \rho_{o,sen}, |\alpha'| \leq \tfrac{\pi}{2}\}, \\ \mathbf{R}_{TB} &\triangleq \{\mathbf{p}' | \rho_{o,safe} < \rho' \leq \rho_{o,sen}, |\alpha'| > \tfrac{\pi}{2}\}, \\ \mathbf{R}_{SF} &\triangleq \{\mathbf{p}' | \rho' \leq \rho_{o,safe}, |\alpha'| \leq \tfrac{\pi}{2}\}, \\ \mathbf{R}_{SB} &\triangleq \{\mathbf{p}' | \rho' \leq \rho_{o,safe}, |\alpha'| > \tfrac{\pi}{2}\},\end{aligned}$$

where $\mathbf{p}' = [x', y']^T$, $\rho' = \|\mathbf{p}' - \mathbf{p}_F\|$, $\alpha' = \text{atan2}(\tilde{y}', \tilde{x}')$, $\begin{bmatrix} \tilde{x}' \\ \tilde{y}' \end{bmatrix} = \begin{bmatrix} \cos\theta_F & \sin\theta_F \\ -\sin\theta_F & \cos\theta_F \end{bmatrix} \begin{bmatrix} x' - x_F \\ y' - y_F \end{bmatrix}$, $\rho_{o,sen}$ and $\rho_{o,safe}$ are the sensitive and safe range for obstacle avoidance respectively. Fig. 1(c) illustrates an example where the nearest obstacle is detected in $\mathbf{R}_{TF}$.

To avoid any potential collision with an obstacle ahead, the instinctive reaction of a human driver is to steer the car away from the obstacle. Inspired by this, our algorithm adopts a steering strategy on the basis of the relative position of the detected obstacles. To facilitate the derivation of the obstacle avoidance algorithm, a bounded barrier function is introduced as follows to describe the obstacle bearing angle constraint.

$$B_{\alpha_o} = \begin{cases} \beta_{\alpha_o} \frac{(\alpha_o - \alpha_{od})^2}{{\alpha_{od}}^2}, & 0 < \alpha_o \leq \alpha_{od} \\ \beta_{\alpha_o} \frac{(\alpha_o + \alpha_{od})^2}{{\alpha_{od}}^2}, & -\alpha_{od} \leq \alpha \leq 0 \end{cases},$$

where α_o is the bearing angle of the nearest obstacle with respect to $\{F\}$, β_{α_o} is a designed parameter and α_{od} represents the critical bearing angle. The introduction of B_{α_o} is to help design an avoidance control law that will drive F to move away from the obstacle. Essentially, the controller should try to steer F such that $|\alpha_o|$ is larger than α_{od}. Generally, $\alpha_{od} = \frac{\pi}{2}$ because under this condition, F will move away from the obstacle with a positive v_F. In experiments, however, α_{od} should be assigned a value larger than $\frac{\pi}{2}$, due to friction and mechanical disturbances.

Based on the definitions given above, a multi-region obstacle avoidance algorithm is proposed in Algorithm 1. In this algorithm, the control input is composed of two parts, namely the leader tracking part and the obstacle avoidance part, where $v_{F,t}$ and $v_{F,a}$ are the leader tracking and obstacle avoidance linear velocities respectively, while $\omega_{F,t}$ and $\omega_{F,a}$ are the leader tracking and obstacle avoidance angular velocities respectively. These control input parts are designed as

follows.

$$
\begin{aligned}
&v_{F,t} = \tfrac{1}{\cos\alpha}[k_\rho \nabla B_\rho + \bar{v}_L \tanh(\tfrac{\bar{v}_L \nabla B_\rho}{\delta_\rho})],\\
&\omega_{F,t} = \tfrac{v_F}{\rho}\sin\alpha + \tfrac{\bar{v}_L}{\rho}\tanh(\tfrac{\bar{v}_L \nabla B_\alpha}{\rho\delta_\alpha}) + k_\alpha \nabla B_\alpha,\\
&v_{F,a} = v_{avoid},\\
&\omega_{F,a} = k_{\alpha_o}\nabla B_{\alpha_o},
\end{aligned}
$$

where v_{avoid} is a positive constant, k_{α_o} is a positive design parameter and ∇B_{α_o} is the gradient of B_{α_o} with respect to α_o. Besides, the control parameters satisfy $|v_{avoid}| \leq \bar{v}_F,\ k_{\alpha_o} \leq \frac{\bar{\omega}_F}{G_{\alpha_o}}$, where $G_{\alpha_o} = \frac{2\beta_{\alpha_o}}{\alpha_{od}}$.

Algorithm 1 Multi-region obstacle avoidance algorithm

Input:
ρ_o, α_o.
Output:
v_F, ω_F.
switch (Region where the obstacle is located)
case $\mathbf{R}_{TF}$**:**
  $v_F = v_{F,t}$, $\omega_F = \min\{\omega_{F,t} + \omega_{F,a}, \bar{\omega}_F\}$.
case $\mathbf{R}_{TB}$**:**
  $v_F = v_{F,t}$, $\omega_F = \omega_{F,t}$.
case $\mathbf{R}_{SF}$**:**
  $v_F = 0$, $\omega_F = \omega_{F,a}$.
case $\mathbf{R}_{SB}$**:**
  $v_F = v_{F,a}$, $\omega_F = 0$.
default:
  $v_F = v_{F,t}$, $\omega_F = \omega_{F,t}$.
end switch

It can be concluded from the algorithm that when ρ_o is larger than $\rho_{o,sen}$, which means that the obstacle does not threaten the safety of F, the leader tracking objective is given the top priority and obstacle avoidance is not activated. When in $\mathbf{R}_{TF}$, the obstacle locates in front of F with ρ_o smaller than $\rho_{o,sen}$ but larger than $\rho_{o,safe}$. In this region, v_F remains identical to $v_{F,t}$, while ω_F is the combination of $\omega_{F,t}$ and $\omega_{F,a}$. Such a reaction helps F try to achieve the leader tracking and obstacle avoidance objectives simultaneously. While in $\mathbf{R}_{TB}$, the obstacle locates behind F. Under this situation, F need not consider the obstacle avoidance objective. In $\mathbf{R}_{SF}$, ρ_o is smaller than $\rho_{o,safe}$. In this region, F stops and rotates so that the obstacle transfers to $\mathbf{R}_{SB}$, where F maintains its heading angle and moves away. From the analysis above, it can be found that using the proposed algorithm, ρ_o is kept greater than or equal to $\rho_{o,safe}$ such that obstacle avoidance can be guaranteed. In addition, it can be easily verified that the control input constraints are satisfied as well.

C. Leader-loss reaction

This subsection will study the leader-loss situation and design a fault-tolerant strategy for tackling this problem. The basic flow of the proposed strategy is presented in Algorithm 2.

Algorithm 2 Fault-tolerant strategy for leader-loss situation

Input:
$({}^T\mathbf{p}_L(t_l), {}^T\theta_L(t_l))$, $({}^T\mathbf{p}_F(t_l), {}^T\theta_F(t_l))$, ρ_o, α_o.
Output:
v_F, ω_F.
1: Plan the shortest path ${}^T\mathbf{p}_V(l)$ from $({}^T\mathbf{p}_F(t_l), {}^T\theta_F(t_l))$ to $({}^T\mathbf{p}_L(t_l), {}^T\theta_L(t_l))$;
2: Design the path following control part $v_{F,p}$ and $\omega_{F,p}$ to drive F moving along ${}^T\mathbf{p}_V(l)$;
3: Design the control law v_F and ω_F using Algorithm 1.

The first step of the proposed fault-tolerant strategy is to solve a shortest path plan problem. According to [19], the shortest path with a constraint on a maximum curvature takes the form of CSC, where C denotes a circular arc with minimum turning radius and S denotes a straight-line segment. As the minimum turning radius of the robot considered in this brief is zero, the shortest path between $({}^T\mathbf{p}_F(t_l), {}^T\theta_F(t_l))$ and $({}^T\mathbf{p}_L(t_l), {}^T\theta_L(t_l))$ is merely a straight line connecting ${}^T\mathbf{p}_F(t_l)$ and ${}^T\mathbf{p}_L(t_l)$.

Next, the control law for driving F to move along the planned path to the goal point should be designed, while the obstacle avoidance and control input constraints should also be guaranteed. Similar to the control scheme proposed in Section III-B, the overall control input is also composed of two parts, which are path following part and obstacle avoidance part. The obstacle avoidance part is the same as that in Section III-B. In the sequel, we mainly focus on the path following part.

The path following control method adopted in this brief is based on the control law proposed in [20]. Similarly, a virtual target is introduced which moves along the path depicted in Fig. 1(b). To facilitate the discussion, the following definitions are given. ${}^T\mathbf{p}_F = [{}^Tx_F, {}^Ty_F]^T$ and ${}^T\theta_F$ are the position and heading angle of F in $\{T\}$, respectively, while ${}^T\mathbf{p}_V = [{}^Tx_V, {}^Ty_V]^T$ and ${}^T\theta_V$ are the position and heading angle of the virtual target in $\{T\}$, respectively. ${}^V\mathbf{p}_F = [{}^Vx_F, {}^Vy_F]^T$ and ${}^V\theta_F$ are the position and heading angle of F in $\{V\}$, respectively, where $\{V\} = \{\vec{x}_V, \vec{y}_V\}$ is the coordinate frame attached on the virtual target as shown in Fig. 1(b). Similar with [20], the path following error dynamics can be derived as follows.

$${}^V\dot{x}_F = -\dot{l} + v_{F,p}\cos{}^V\theta_F,\ {}^V\dot{y}_F = v_{F,p}\sin{}^V\theta_F,\ {}^V\dot{\theta}_F = \omega_{F,p},$$

where ${}^V\theta_F = {}^T\theta_F - {}^T\theta_V$.

To drive F moving along the path, let the rate of progression of the virtual target along the planned path be governed by

$$\dot{l} = v_{F,p}\cos{}^T\theta_F + k_1{}^Vx_F, \tag{11}$$

where k_1 is a positive constant parameter. Then, the path following control law is designed as follows.

$$
\begin{aligned}
v_{F,p} =& v_{follow},\\
\omega_{F,p} =& \dot{\delta} - \gamma\tanh({}^Vy_F)[1-\tanh^2({}^Vy_F)]v_{F,p}\frac{\sin{}^V\theta_F - \sin\delta}{{}^V\theta_F - \delta},\\
&- k_2\tanh({}^V\theta_F - \delta)
\end{aligned} \tag{12}
$$

where k_2 and γ are positive constant parameters, v_{follow} is a positive constant, which means that F moves at a constant speed along the path, and δ is the expected transient maneuver, which is given as $\delta = -\theta_\delta\tanh(\beta_\delta{}^Vy_F)$, where θ_δ and β_δ are

positive design parameters. In addition, the parameters of (12) should satisfy the following conditions.

$$v_{follow} \leq \bar{v}_F,\ k_2 + \theta_\delta \beta_\delta v_{F,p} + \frac{2\sqrt{3}}{9}\gamma v_{F,p} \leq \bar{\omega}_F. \quad (13)$$

It can be proven that based on the proposed path following control law (11) and (12), ${}^V\mathbf{p}_F$ and ${}^V\theta_F$ will converge to zero asymptotically. A formal statement of this result is presented in the following theorem.

Theorem 2. *Consider a robot modeled by (1) and a desired path ${}^T\mathbf{p}_V(l)$ parameterized by l. The control law (11) and (12) ensure that ${}^Vx_F$, ${}^Vy_F$ and ${}^V\theta_F$ are bounded, while ${}^V\mathbf{p}_F$ and ${}^V\theta_F$ converge to zero asymptotically. In addition, control input constraints (6) are satisfied.*

Proof: Consider the following Lyapunov function candidate.

$$V = \frac{1}{2}{}^Vx_F^2 + \frac{1}{2}\tanh^2({}^Vy_F) + \frac{1}{2\gamma}{}^V\theta_F^2. \quad (14)$$

Differentiating (14) with respect to time and combining with (11) and (12) yields

$$\begin{aligned}\dot{V} = &-k_1{}^Vx_F^2 + \tanh({}^Vy_F)[1-\tanh^2({}^Vy_F)]v_{F,p}\sin\delta \\ &- \frac{k_2}{\gamma}({}^V\theta_F - \delta)\tanh({}^V\theta_F - \delta)\end{aligned}.$$

According to the definition of δ and the fact that $\sin(\cdot)$ and $\tanh(\cdot)$ are both odd, $\tanh({}^Vy_F)\sin\delta \leq 0$. Besides, as $v_{F,p} > 0$ and $\tanh(x) \in (-1,1)$, it can be obtained that $\tanh({}^Vy_F)[1-\tanh^2({}^Vy_F)]v_{F,p}\sin\delta \leq 0$. Therefore, $\dot{V} \leq 0$. From (14), it can be concluded that ${}^Vx_F$, ${}^Vy_F$ and ${}^V\theta_F$ are all bounded. It can also be obtained that $E = \{{}^V\mathbf{p}_F, {}^V\theta_F | \dot{V} = 0\} = \{{}^V\mathbf{p}_F = \mathbf{0}, {}^V\theta_F = 0\}$, which is an invariant set. Thus, the maximum invariant set in E is itself. According to the LaSalle's invariance principle [21], ${}^V\mathbf{p}_F$ and ${}^V\theta_F$ will asymptotically converge to zero.

Next, the input constraints are discussed. According to Lemma 1 and 2, it can be derived that $|\omega_{F,p}| \leq \left|\dot{\delta}\right| + k_2 + \frac{2\sqrt{3}}{9}\gamma v_{F,p}$. As $\dot{\delta} = -\theta_\delta[1-\tanh^2(\beta_\delta{}^Vy_F)]\beta_\delta{}^V\dot{y}_F$, $\left|\dot{\delta}\right| \leq \theta_\delta\beta_\delta v_{F,p}$. Therefore, $|\omega_{F,p}| \leq \theta_\delta\beta_\delta v_{F,p} + k_2 + \frac{2\sqrt{3}}{9}\gamma v_{F,p}$. According to the parameter selection condition (13), control input constraints are satisfied.

Thus, the proof completes. ■

IV. Experiment Results

The presented approach has been implemented on a multi-robot system consisting of two Pioneer 3-AT mobile robot platforms as depicted in Fig. 2(a). L robot was equipped with a Dell Precision M2800 Mobile Workstation and a Hokuyo UTM-30LX Scanning Laser Rangefinder, while F robot was equipped with a ZOTAC ZBOX-VR7N70 mobile PC, a ZED stereo camera and a Hokuyo UTM-30LX Scanning Laser Rangefinder. The algorithms were programmed using C++ language under Robotic Operating System (ROS), Kinetic release. In the experiment, L robot moved autonomously in the workspace and our proposed method was applied to F robot.

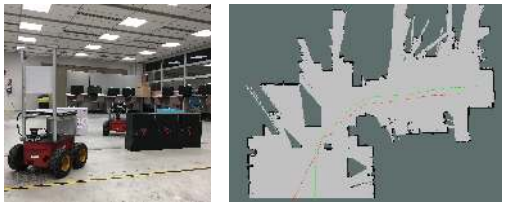

(a) Experiment setup (b) Map and robot paths

Fig. 2. Experiment setup, map and robot paths

In the experiment, the control period was set as 0.03s. The parameters of system constraints were set as $\rho_{min} = 1$m, $\rho_{max} = 3$m, $\alpha_{min} = -35°$, $\alpha_{max} = 35°$, $\rho_{o,safe} = 0.5$m, $\bar{v}_L = 0.3$m/s, $\bar{\omega}_L = 2$rad/s, $\bar{v}_F = 0.7$m/s and $\bar{\omega}_F = 2$rad/s. The control parameters for leader tracking were designed as $\rho_d = 1.5$m, $\alpha_d = 0°$, $\beta_\rho = 10$, $\beta_\alpha = 1$, $k_\rho = 0.0068$, $\delta_\rho = 0.35$, $k_\alpha = 0.39$ and $\delta_\alpha = 0.1$. The control parameters for unknown obstacle avoidance were set as $\rho_{o,sen} = 0.9$m, $\beta_{\alpha o} = 1$, $k_{\alpha o} = 1$, $\alpha_{od} = 120°$ and $v_{avoid} = 0.3$m/s. The control parameters for the leader-loss reaction were designed as $k_1 = 1$, $k_2 = 1$, $\gamma = 1$, $v_{follow} = 0.3$m, $\theta_\delta = \frac{\pi}{2}$ and $\beta_\delta = 1$.

In the experiment, L moved from a room with many unknown obstacles to another room through a door autonomously. F tracked L while performing obstacle avoidance simultaneously. Fig. 2(b) depicts the map of the environment and the paths of two robots, where the green one denotes the leader path and the red one is the path of F. It should be noted that the map is only used to help exhibit the experiment results vividly, which was generated by L using the SLAM technique, while F did not utilize the map information for control. Fig. 3(a) shows ρ during operation while Fig. 3(b) describes α. From these two figures and also Fig. 2(b), it can be found that when the robots arrived at the second room without obstacles nearby, ρ and α both converged into the respective designed sets, which indicates that the proposed leader tracking control law is capable of controlling F to track L with a flexible formation structure. It can be revealed from Fig. 3(a) and 3(b) that F first detected L at about 38s and leader-loss situation happened frequently from 50s to 70s, which may be caused by obstacle avoidance behavior, illumination disturbance or motion blurring. Even though L was lost frequently, F managed to re-detect it and recover tracking, which demonstrates the effectiveness of the proposed fault-tolerant strategy. Fig. 3(c) and Fig. 3(d) describe ρ_o and α_o respectively. These two figures show that between 47s and 64s, there were obstacles located within $\rho_{o,sen}$ and thus the obstacle avoidance algorithm was activated. Based on these two figures, it can be concluded that F succeeded in avoiding the obstacles. At about 51s, ρ_o was a little smaller than 0.5m, which can be explained by inertia of the robot despite zero input velocity. The obstacle avoidance can also be observed directly from Fig. 2(b), in which F successfully avoided densely distributed obstacles when moving from the first room to the other. Fig. 3(e) and 3(f) depict v_F and ω_F respectively. From these two figures, it can be concluded that the control input constraints were satisfied. Before 75s, the

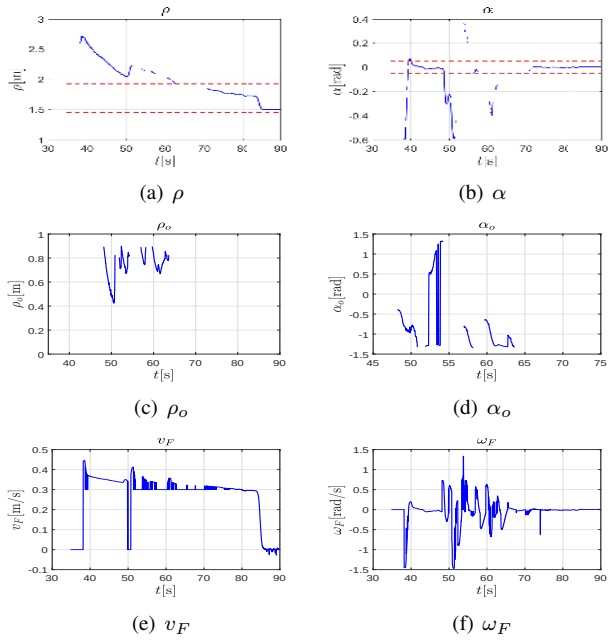

(a) ρ (b) α

(c) ρ_o (d) α_o

(e) v_F (f) ω_F

Fig. 3. Experiment results

control inputs changed dramatically, which was caused by the obstacle avoidance behavior and the leader-loss reaction. After that, the control inputs were smooth.

Remark 1. *In this experiment, each robot obtained the information using its onboard sensor such that they worked in a totally decentralized manner, which is different from the experiments in many similar literatures like [2], where they usually rely on a motion capture system to measure the position and heading angle of each robot in a centralized way to test their decentralized methods.*

V. Conclusions and Future Works

This brief studies the $L-F$ tracking control problem for multiple nonholonomic mobile robots, and a series of practical issues including sensor limitations, obstacle and inter-robot collision avoidance, leader-loss situation, etc., have been explicitly taken into account. The proposed control scheme is under the assumption that global state measurements are not available and there are no communication links among robots, which makes the proposed approach more applicable for practical applications than existing methods. In this brief, sensor limitations and $L-F$ collision avoidance are modeled as distance and bearing angle constraints. To describe these constraints, a bounded barrier function is introduced and incorporated in the leader tracking control law. To guarantee the safety of the robots, a multi-region obstacle avoidance algorithm is designed which prioritizes different objectives in different regions. It is proven that when there are no obstacles nearby, the proposed approach can form a flexible formation structure while distance and bearing angle constraints are not violated. The leader-loss situation has first been considered in this brief. Then a fault-tolerant strategy is proposed when the visibility is broken. Real robot experiment was conducted to demonstrate the effectiveness of the proposed method. This brief primarily focuses on the tracking control problem of a $L-F$ pair. Future work will investigate the extension of the proposed approach to scenarios of multiple followers tracking a common leader, where the collision avoidance is considered a more challenging issue.

References

[1] K.-K. Oh, M.-C. Park, and H.-S. Ahn, "A survey of multi-agent formation control," *Automatica*, vol. 53, pp. 424–440, 2015.

[2] D. Sakai, H. Fukushima, and F. Matsuno, "Leader-follower navigation in obstacle environments while preserving connectivity without data transmission," *IEEE Transactions on Control Systems Technology*, 2017.

[3] M. A. Lewis and K.-H. Tan, "High precision formation control of mobile robots using virtual structures," *Autonomous robots*, vol. 4, no. 4, pp. 387–403, 1997.

[4] T. Balch and R. C. Arkin, "Behavior-based formation control for multirobot teams," *IEEE Transactions on robotics and automation*, vol. 14, no. 6, pp. 926–939, 1998.

[5] C. C. Cheah, S. P. Hou, and J. J. E. Slotine, "Region-based shape control for a swarm of robots," *Automatica*, vol. 45, no. 10, pp. 2406–2411, 2009.

[6] N. Ceccarelli, M. Di Marco, A. Garulli, and A. Giannitrapani, "Collective circular motion of multi-vehicle systems," *Automatica*, vol. 44, no. 12, pp. 3025–3035, 2008.

[7] X. Jin, "Fault tolerant finite-time leader–follower formation control for autonomous surface vessels with los range and angle constraints," *Automatica*, vol. 68, pp. 228–236, 2016.

[8] Y. Wang, D. Wang, and B. C. Ng, "Finite time moving target tracking using nonholonomic vehicles with distance and bearing angle constraints," in *American Control Conference (ACC), 2017*. IEEE, 2017, pp. 2962–2967.

[9] S. Mastellone, D. M. Stipanović, C. R. Graunke, K. A. Intlekofer, and M. W. Spong, "Formation control and collision avoidance for multi-agent non-holonomic systems: Theory and experiments," *The International Journal of Robotics Research*, vol. 27, no. 1, pp. 107–126, 2008.

[10] E. J. Rodríguez-Seda, C. Tang, M. W. Spong, and D. M. Stipanović, "Trajectory tracking with collision avoidance for nonholonomic vehicles with acceleration constraints and limited sensing," *The International Journal of Robotics Research*, vol. 33, no. 12, pp. 1569–1592, 2014.

[11] R. Zheng, Y. Liu, and D. Sun, "Enclosing a target by nonholonomic mobile robots with bearing-only measurements," *Automatica*, vol. 53, pp. 400–407, 2015.

[12] M. Deghat, I. Shames, and B. Anderson, "Safe autonomous agent formation operations via obstacle collision avoidance," *Asian Journal of Control*, vol. 17, no. 5, pp. 1473–1483, 2015.

[13] S. S. Ge, X. Liu, C.-H. Goh, and L. Xu, "Formation tracking control of multiagents in constrained space," *IEEE Transactions on Control Systems Technology*, vol. 24, no. 3, pp. 992–1003, 2016.

[14] Y. Wang, D. Wang, and S. Zhu, "Formation tracking of multi-vehicle systems in unknown environments using a multi-region control scheme," *International Journal of Control*, pp. 1–12, 2016.

[15] N. Léchevin, C. A. Rabbath, and P. Sicard, "Trajectory tracking of leader–follower formations characterized by constant line-of-sight angles," *Automatica*, vol. 42, no. 12, pp. 2131–2141, 2006.

[16] F. Morbidi, F. Bullo, and D. Prattichizzo, "Visibility maintenance via controlled invariance for leader–follower vehicle formations," *Automatica*, vol. 47, no. 5, pp. 1060–1067, 2011.

[17] R. Murrieta-Cid, U. Ruiz, J. L. Marroquin, J.-P. Laumond, and S. Hutchinson, "Tracking an omnidirectional evader with a differential drive robot," *Autonomous Robots*, vol. 31, no. 4, pp. 345–366, 2011.

[18] D. Panagou and V. Kumar, "Cooperative visibility maintenance for leader–follower formations in obstacle environments," *IEEE Transactions on Robotics*, vol. 30, no. 4, pp. 831–844, 2014.

[19] W. Wu, H. Chen, and P.-Y. Woo, "Time optimal path planning for a wheeled mobile robot," *Journal of Field Robotics*, vol. 17, no. 11, pp. 585–591, 2000.

[20] D. Soetanto, L. Lapierre, and A. Pascoal, "Adaptive, non-singular path-following control of dynamic wheeled robots," in *Decision and Control, 2003. Proceedings. 42nd IEEE Conference on*, vol. 2. IEEE, 2003, pp. 1765–1770.

[21] J.-J. E. Slotine, W. Li *et al.*, *Applied nonlinear control*. Prentice hall Englewood Cliffs, NJ, 1991, vol. 199, no. 1.